Bull. Mater. Sci., Vol. 40, No. 6, October 2017, pp. 1213–1224
DOI 10.1007/s12034-017-1466-1

Impact of nano-ZnO/grafted textile on the outer membrane permeability of some pathogenic bacteria

M B EL-ARNAOUTY[1], M EID[1,*] and S Y EL TABLAWY[2]
[1]Polymer Chemistry Department, National Center for Radiation Research and Technology (NCRRT), Atomic Energy Authority, P.O. Box 29, Nasr City, Egypt
[2]Department of Drug Radiation Research, National Center for Radiation Research and Technology (NCRRT), Atomic Energy Authority, P.O. Box 29, Nasr City, Egypt
*Author for correspondence (mona_eid2000@yahoo.com)

MS received 7 March 2016; accepted 10 February 2017; published online 15 September 2017

Abstract. Cotton textile grafted by chitosan hydroxyethyl methacrylate has been prepared by gamma radiation as a polymeric stabilizer for ZnO nanoparticles (NPs). The grafting percent and swelling property of the prepared grafted polymer in bi-distilled water were studied and the results showed that the swelling percent of the plain textile is higher than that of all different compositions. The morphology and structure of plain textile, grafted textile and nano-ZnO/grafted textile were examined by scanning electron microscopy (SEM) and Fourier transform infrared spectroscopy (FT-IR). The presence of ZnO in the prepared samples was examined by energy-dispersive X-ray spectroscopy (EDX) and X-ray diffraction (XRD). The particle size of the formed ZnO NPs has been estimated by transmission electron microscopy (TEM). The results indicate the nanoscale of the ZnO particles. Nano-ZnO/grafted textile was tested against some pathogenic strains, and the results show that the nano-ZnO/grafted textile was able to attenuate bacterial growth of *MRSA* and *Klebsiella pneumoniae* after 24 h of direct contact. Also, release of potassium ions, loss of absorbing materials and decrease of membrane surface potential were noticed, indicating alteration of cell membrane permeability. Furthermore, SEM observation showed bacterial cell deformation for growth on the nano-ZnO/grafted textile. These results have been promising in the antibacterial field.

Keywords. Textile; chitosan; HEMA; ZnO nanoparticles; FTIR; pathogenic bacteria.

1. Introduction

There has been a great deal of attention in recent years given to the hazards of microbial contamination from potential everyday exposure, especially in hospitals (nosocomial infection). A wide range of bacteria, fungi and viral pathogens are responsible for such infections. A rapid and uncontrolled multiplication of these pathogenic microbes can seriously compromise health and hygienic living standards. One potential method for reducing the occurrence and spread of nosocomial infections is the use of antimicrobial textiles. Textiles of all varieties are considered to be very proficient at carrying bacteria and serving as a reservoir for the transmission of infection [1]. Textiles from natural fibres such as cotton are also well known to be more susceptible to microorganisms than synthetic fibres because they are capable of easily holding water, oxygen and nutrients, providing a favourable environment for bacterial growth [2]. Therefore, antimicrobial textiles may be of great help in the recovery process of transplant patients, people with immunodeficiency diseases, low-immunity patients and premature babies [1]. Two different aspects of antimicrobial protection provided by chemical finishes can be distinguished. The first is the protection of the textile user against pathogenic or odour-causing microorganisms. The second is the protection of the textile fibres itself, from degradation [3]. Chitosan exhibits excellent biological properties; it is nontoxic, biocompatible and biodegradable [4]. For its exceptional features, chitosan has received interest in various fields.

Inorganic materials such as metal oxides attracted a great attention over the past decade owing to their ability to withstand harsh process conditions [5,6]. Organic materials and metal oxides such as TiO_2, ZnO, MgO and CaO are of special interest as they are not only stable under harsh process conditions but also generally regarded as safe materials to human beings and animals [5,7]. Nanoparticles (NPs) with their large surface area to volume ratio have been studied as likely candidates for antimicrobial agents. The antimicrobial activity has been observed to vary as a function of surface area in contact with the microbe; therefore, NPs with large surface area ensure a broad range of reactions with the bacterial surface [8]. Metal oxide NPs with antimicrobial activity, when embedded and coated on to surfaces, can find immense applications in numerous fields such as water treatment, cosmetics, synthetic textiles, biomedical and surgical devices [9]. These inorganic NPs kill bacteria through various mechanisms, e.g., binding to intracellular proteins and inactivating them, generation of reactive oxygen and via direct damage to cell walls [10]. Microbes are more unlikely to develop resistance against

NPs since they attack a broad range of targets, which requires the microorganism to develop defence mechanisms.

Nano-ZnO/grafted textiles have become quite common [11,12]. To our knowledge, the efficiency of ZnO NP in imparting antibacterial effect to fabric is not yet well established although it is known to have a strong resistance to microorganisms [12]. ZnO NP is currently being investigated as an antibacterial agent both against Gram-negative microorganisms such as *Escherichia coli* and Gram-positive microorganisms such as *Staphylococcus aureus* in microscale and nanoscale formulations [13]. An important aspect of the use of ZnO as antibacterial agent is the requirement that the particles are not toxic to human cells [14,15].

In the present work a simple method is suggested to develop a medical fabric using nano-ZnO/cotton textile grafted by chitosan/2-hydroxyethylmethacrylate (HEMA) [textile-g-(chitosan/HEMA)] using gamma radiation to evaluate the antibacterial properties and the proposed mechanism of action of this antibacterial agent. The prepared polymeric nanocomposites were evaluated by infrared (FT-IR) spectroscopy, scanning electron microscopy (SEM), energy-dispersive X-ray spectroscopy (EDX), X-ray diffraction (XRD) and transmission electron microscopy (TEM).

2. Experimental

2.1 *Chemicals*

HEMA of purity 99% (Merck, Germany) was used as received. Chitosan [molecular weight 100,000–300,000, $(C_6H_{11}NO_4)_n$] was obtained from Acros Organics (New Jersey, USA, and Geel, Belgium). ZnO NP (Mw 81.39 g mol^{-1}, powder NP size < 50 nm) was obtained from Sigma-Aldrich (Germany).

2.2 *Preparation of nano-ZnO/[textile-g-(chitosan/HEMA)]*

Aqueous solutions of 2% chitosan and 50% HEMA were mixed in different ratios of (chitosan/HEMA)—(20:80), (40:60), (50:50), (60:40) and (80:20). The mixtures were poured into test tubes of diameter 15 mm containing 6×5 cm^2 textile samples of known weight and irradiated with gamma rays using a cobalt-60 source at radiation dose of 20 kGy. After irradiation, the grafted textile samples were washed thoroughly with hot distilled water and soaked overnight in water to extract the residual monomer and homopolymer. The samples were then dried in a vacuum oven at 40°C for 24 h and weighed. The degree of grafting (%) was determined by the percentage increase in weight as follows:

$$\text{Grafting } (\%) = [(W_g - W_o)/W_o] \times 100, \quad (1)$$

where W_o and W_g represent the weight of ungrafted and grafted sample, respectively.

To prepare nano-ZnO/textile-g-(chitosan/HEMA), the grafted textile samples were immersed in different concentration of aqueous ZnO solution for 24 h, dried and stored for later use.

2.3 *Swelling studies*

For swelling studies, pre-weighed grafted textile samples were immersed into bi-distilled water. Swollen grafted textile sample were removed from water at regular intervals and dried superficially with filter paper, weighed and placed in the same bath. Swelling (%) was calculated as follows:

$$\text{Swelling } (\%) = [(W_s - W_o)/W_o] \times 100, \quad (2)$$

where W_s is the weight of the swollen grafted textile and W_o is the weight of initial dry sample.

2.4 *Characterization*

FT-IR of grafted textile samples was performed according to ASTM E 1252-(02) 'Standard Practice for General Techniques for Obtaining Infrared Spectra using Perkin-Elmer Spectrum One (USA)' in the range 400–4000 cm^{-1}. A scanning electron microscope (JEOL-JSM-5400, Japan) was used for investigating the surface morphology of the plain, grafted and nano-ZnO/grafted textile samples at a high magnification and resolution by means of an energetic electron beam. EDX measurements of nano-ZnO/grafted textile samples were characterized using an EDX (Oxford, England)-ISIS attached to a SEM-JEOL-5400 with voltage of 20 keV. The XRD method was used to identify the ZnO NPs in the grafted textile nanocomposites. These measurements were carried out using a Shimadzu X-ray diffractometer (XRD-6000 model) equipped with an X-ray tube [Cu target, 40 kV (voltage), 30 mA (current)]. The X-ray data were recorded in the 2θ range 4–90° (degree) with continuous scanning mode and scanning speed 8° min^{-1}. A transmission electron microscope (TEM) was used to image the ZnO nanocomposites. Finely ground nano-ZnO/grafted textile samples were dispersed in 1 ml of ethanol followed by sonication to get a solution of ZnO NPs. Approximately 10–20 µl of this solution was dropped on a 3 mm copper grid and dried at room temperature. The copper grid was inserted into the TEM.

2.5 *Microbiological studies*

A total of 20 preliminary identified clinical isolates (5 *Staphylococcus* spp., 5 *Escherichia coli*, 5 *Klebsiella* spp., 3 *Pseudomonas* spp., 1 *Bacillus* sp. and 1 *Candida* sp.) were obtained from the Drug Microbiology Laboratory, Drug Radiation Research Department. Cultures were grown on nutrient agar (NA) plates and Sabouraud-Dextrose agar (SDA) for *Candida* sp. and maintained in the agar slants at 4°C. The antibacterial activity of nano-ZnO/grafted textile with different concentrations of ZnO was tested qualitatively and quantitatively.

Qualitative assessment of antibacterial activity was assayed using the disk diffusion method as described by Ophori and Wemabu [16]. Briefly, a small single isolated colony was emulsified in 2 ml sterile nutrient broth (NB) or Sabouraud-Dextrose broth (SDB) and incubated at 37°C for 3 h. Sterile cotton swabs with the suspensions were used to evenly spread the entire surface of Mueller–Hinton agar plates to obtain uniform inocula. The plates were dried for 2–4 min. Discs (5 mm diameter) of the plain, the grafted and the nano-ZnO/grafted textile samples (pre-sterilized by autoclaving at 121°C for 15 min) were gently pressed onto the surface of the plate. The plates were incubated at 37°C for 24 h. The antibacterial activity of the tested fabrics was demonstrated by the diameter of the zone of inhibition in comparison with the plain one. The experiment was performed in duplicate and the mean value was taken. The most susceptible isolates were identified according to their macroscopic and microscopic morphology and genetically identified by ribosomal ribonucleic acid (rRNA). To study the molecular identification, bacterial whole genomes were extracted using a Wizard genomic DNA isolation kit (#A1120, Promega Corporation, USA). Bacterial identification by PCR and direct sequencing of 16S rRNA gene were performed according to [17], using forward 8F primer '5′ AGA GTT TCC TGG CTC AG' and reverse U1492R primer '5′GGT TAC CTT GTT ACG ACT T'. It was applied in Centre of Virology, Faculty of Agriculture, Cairo University.

Quantitative measurement of antibacterial activity was carried out according to the AATCC Test Method [18]. The tested textile disc was placed in a sterile screw-capped tube; 100 μl of 10^6 CFU ml^{-1} from the different tested bacterial strains was loaded on it with even distribution of the inocula. At different time intervals (2, 4, 6 and 24 h), 900 μl of sterile distilled water was added and mixed by shaking for 1 min. After that, 10-fold dilutions in sterile distilled water were made. From each dilution, 100 μl was surface inoculated on NA plates. Then, the plates were incubated at 37°C for 24 h. Colonies were counted and the reduction percent ($R\%$) was calculated using the following equation:

$$R(\%) = (B - A) \times 100/B,$$

where A is the number of bacterial colonies from the treated disc after the contact period and B is the number of bacterial colonies from plain discs at zero contact time.

2.6 *Microbiological assays*

To estimate the potassium ion leakage, overnight NB cultures of the tested cells were centrifuged and the cells were washed three times by deionized water. Then, the cells were re-suspended in 5 ml of sterilized deionized water and treated with discs of nano-ZnO/grafted textile. They were incubated at 37°C for 30, 60 and 120 min and the levels of K^+ ions were measured using a photometer (Alfa Wasserman Style 111, Na^+, K^+, Cl^- analyser). Flasks with plain discs were tested similarly. Results were expressed as the amount of extracellular free potassium (mmol l^{-1}) in the growth media in each interval of incubation period [19]. To measure the release of 260 nm absorbing material from cells treated by plain textile and nano-ZnO/grafted textile discs, the discs were added to 2 ml of 18 h bacterial culture in sterile peptone water. After incubation at 35°C for 2, 4 and 6 h, cells were centrifuged at 3,500 rpm and the optical densities (ODs) of the supernatants were measured spectrophotometrically using a JASCO V 560 UV–VIS spectrophotometer at 260 nm to observe the bacterial cell damage.

The surface charge of the cells under study was evaluated and measured as zeta potential. The zeta potential of bacterial cultures, treated with plain textile discs or with nano–ZnO/grafted textile discs, was measured using a Nano Zeta Potential/Particle Sizer NICOMP™ 380 ZLS PSS (Nicomp Particle Sizing System, Santa Barbara, California, USA). Briefly,100 μl of the bacterial culture was freshly inoculated in 5 ml of MHB and incubated at 37°C for 360 min, where final bacterial concentration of ≈1.1×10^9 CFU ml^{-1} was reached (0.4 at OD 590). The bacterial suspensions were then centrifuged at 10,000 rpm (20 min), the supernatant was discarded and the cell pellets were washed five times with 0.5 mM potassium phosphate buffer solution (pH 7.4). The bacterial cell suspension was prepared by re-suspending the

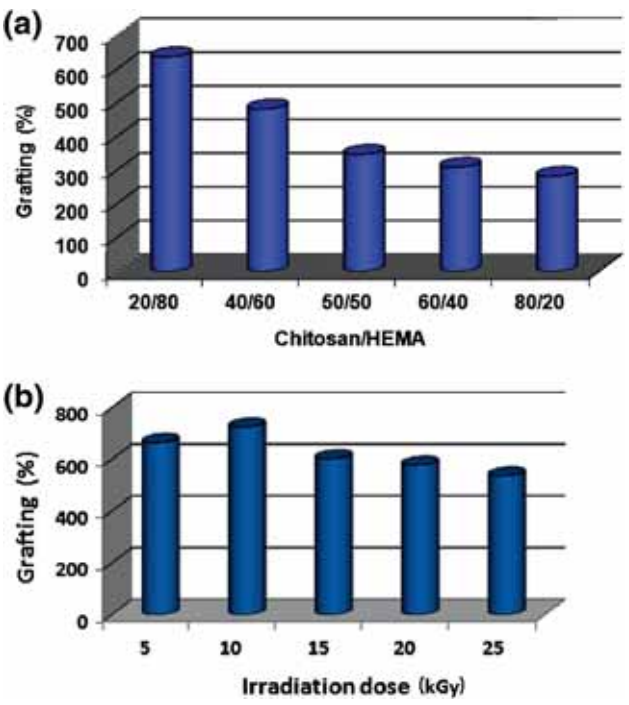

Figure 1. (**a**) Effect of copolymer composition on the grafting (%) of textile-g-(chitosan/HEMA) prepared by gamma irradiation at 20 kGy. (**b**) The effect of irradiation dose on the grafting (%) of textile-g-(chitosan/HEMA) (50:50).

cell pellet in the used buffer. The OD 590 of the final dispersion varied between 0.12 and 0.15; then the washed bacterial cell suspension was incubated with discs of nano-ZnO/grafted textiles and incubated for 1 h at room temperature prior to zeta potential measurements. For the positive control, the washed bacterial cell pellets were incubated at the same conditions without nano-ZnO treatment [20]. For SEM study, plain textile and nano-ZnO/grafted textile discs were placed on NA plates seeded with 100 µl of the tested strain. The plates were incubated at 37°C for 24 h; later small parts of the discs were cut, directly coated using a gold sputter coater and examined using A JEOL-JSM-5400 (Japan) scanning electron microscope.

3. Results and discussion

Figure 1a and b shows the effect of copolymer composition and irradiation dose on the grafting (%) of textile-g-(chitosan/HEMA) prepared by gamma radiation. As shown in figure 1a, the copolymer composition significantly influences the degree of grafting (%) of the grafted textile. It is clear from the figure that the grafting percentage highly increases by increasing HEMA content. The afore-mentioned results could be explained in the light of increasing of vinyl groups present in the copolymer that was prepared with a high content of HEMA [21]. This may be due to the higher diffusivity of the HEMA into the textile matrix compared with that of chitosan. Also the grafting process of (chitosan/HEMA) copolymer composition may be enhanced in the presence of HEMA due to its higher polarity strength than that of chitosan [22].

The effect of the irradiation dose on the grafting (%) of textile-g-(chitosan/HEMA) is shown in figure 1b. From the figure it can be noticed that the grafting (%) increases at irradiation dose of 10 kGy. This may be due to an increase in the number of free radicals formed, which increases the diffusion rate of copolymer into the textile matrix, thus increasing the grafting yield [23]. It was also noticed that at irradiation doses higher than 10 kGy, the degree of grafting (%) decreased; this is due to the increase of the free

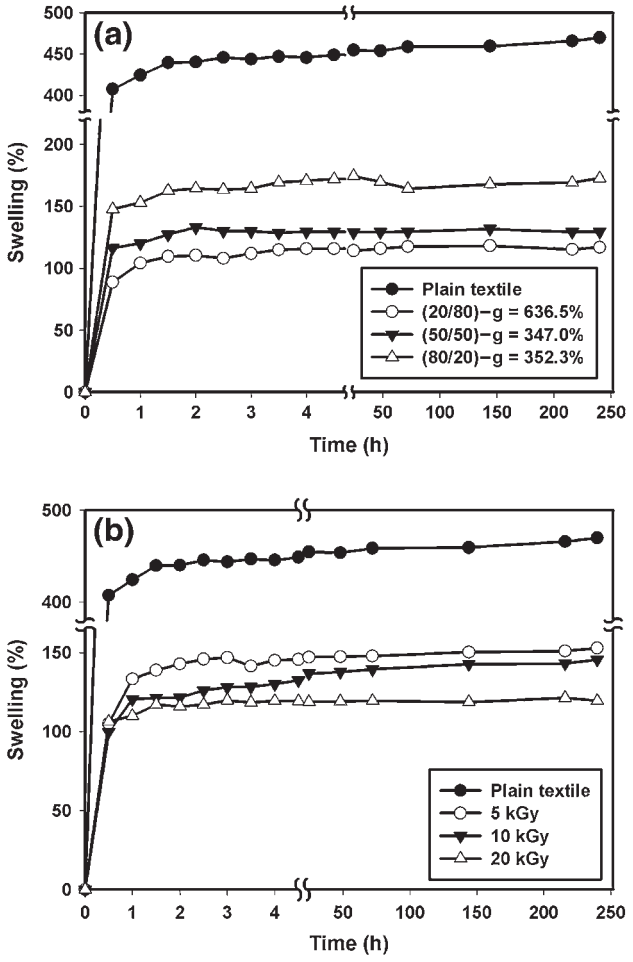

Figure 2. (**a**) Effect of copolymer composition on the swelling (%) of textile-g-(chitosan/HEMA) prepared by gamma irradiation 20 kGy. (**b**) The effect of irradiation dose on the swelling (%) of textile-g-(chitosan/HEMA) (50:50).

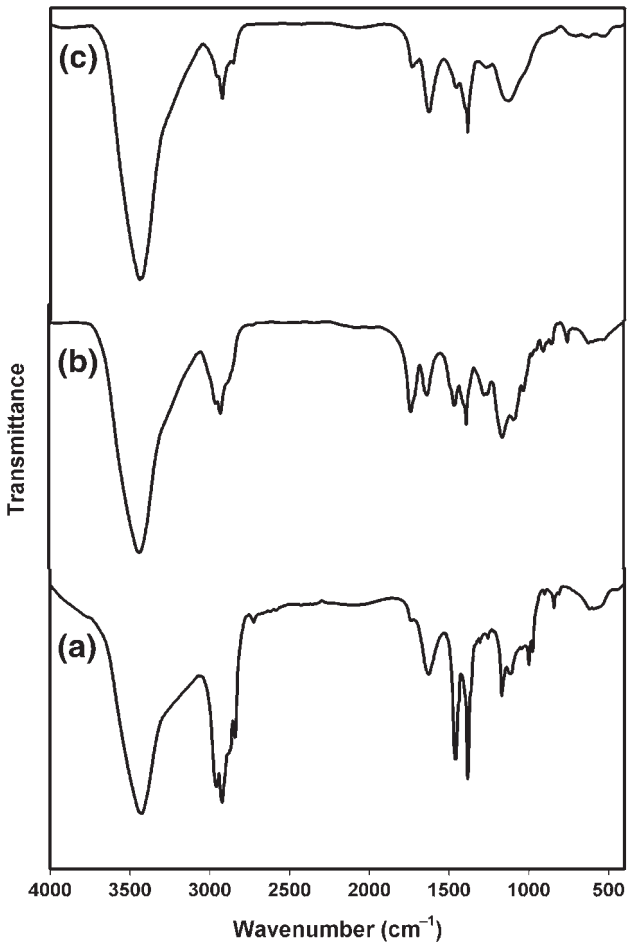

Figure 3. FTIR spectra of (**a**) plain textile, (**b**) textile-g-(chitosan/HEMA) and (**c**) nano-ZnO/grafted textile at 20 kGy.

radicals numbers, which leads to recombination of the free radicals with each other and the rapid formation of the homopolymer rather than the diffusion into the textile matrix [24].

3.1 *Swelling study*

When a grafted textile is brought into contact with water, the solution diffuses into the network and a volume phase transition occurs, resulting in the expansion of the grafted textile. Diffusion involves the migration of fluid into the grafted textile or dynamically formed spaces between the grafted textile chains. Swelling of the grafted textile involves a large segmental motion, resulting, ultimately, in the increased separation of the grafted textile chains [25]. The effect of the copolymer composition on the swelling percent is presented in figure 2a. It can be seen that the swelling behaviour of the grafted textile is greatly influenced by its composition. The figure shows that the swelling percent of grafted textile decrease by increasing HEMA content in the feed mixture. It would hold the network perfectly by increasing the crosslinking density as the free radicals increase it also resulted in the narrowing of pore size and reduce the free space available for water retention [26].

It is well known that the degrees of grafting and crosslinking greatly depend on the irradiation dose. Higher exposure dose means a longer exposure time, which consequently prolongs the propagation step of the process of copolymerization leading to higher degrees of conversion and crosslinking. The effect of irradiation dose on the swelling of grafted textile is shown in figure 2b. From the figure, it is found that the swelling (%) decreases as the irradiation dose increases, which may be due to the increasing of the crosslinking percentage in the grafted textile. As a result, a reduction of the free volume available for swelling by increasing the tightness of the network structure will happen.

3.2 *Characterization*

Compositional and structural information concerning plain textile, textile-g-chitosan/HEMA and nano-ZnO/grafted textile samples has been investigated by FTIR spectroscopy. Spectra of different samples are shown in figure 3a–c. In the

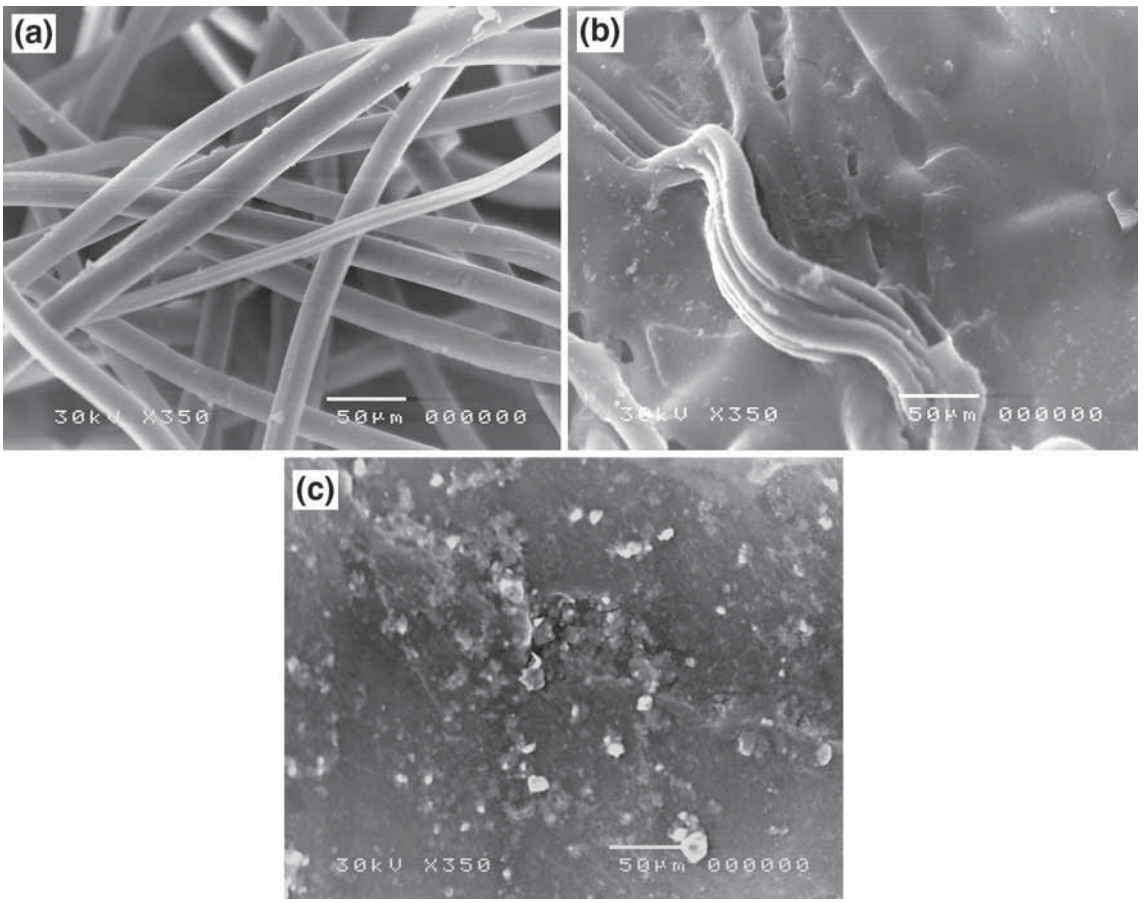

Figure 4. SEM images of (**a**) plain textile, (**b**) textile-g-(chitosan/HEMA) (50:50) and (**c**) nano-ZnO/grafted textile at 20 kGy.

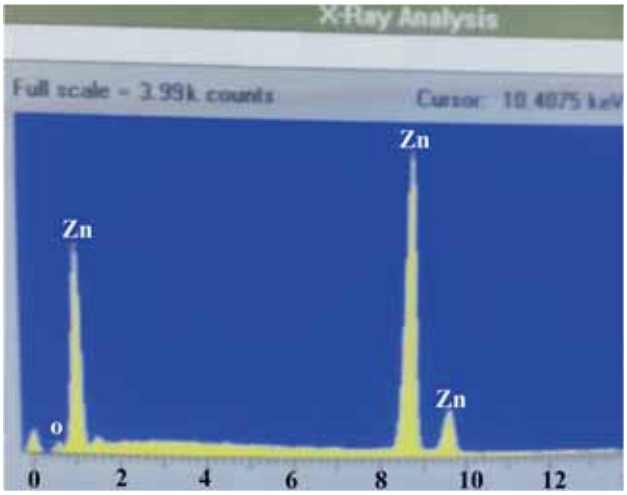

Figure 5. EDX measurement of nano-ZnO/grafted textile at 20 kGy.

spectra of plain textile (figure 3a), the characteristic absorptions that appear at 1156, 1081 and 1019 cm^{-1} are attributed to the C–O–C stretching vibration of the anhydroglucose of cellulose units. The band at 2930 cm^{-1} is characteristic of the CH_3 stretching vibration and the bands at 2850 and 1457 cm^{-1} are attributed to CH_2 [27–29]. Figure 3b, of textile-g-(chitosan/HEMA) spectrum, shows absorption bands for the C=O stretching, and N–H bending of the amide bands appears at 1623 cm^{-1}. The regions of absorption peaks for the N–H stretching of the primary amide appear at 3197 and 3446 cm^{-1}. In addition, the peak at 1400 cm^{-1} is for the –C–N stretching, and at 750 cm^{-1} is for the weak band N–H out-of-plane bending. As shown in figure 3c, the interaction of ZnO NPs with grafted textile results in the decrease of the band intensity of OH and NH and also in the absorption band of C=O [30].

Figure 4a, b and c shows the SEM of the plain textile, the textile-g-(chitosan/HEMA) and the nano-ZnO/grafted textile, respectively. The apparent physical nature of the plain textile, as seen in figure 4a, shows the smooth fibrous network. Figure 4b shows the crosslinking copolymer formed within the plain textile network. The resulting polymer forms a coating of the fibres as shown in the figure, which reveals that the surface is not smooth and many wrinkles are observed. This is probably due to structural rearrangement on the chains of functional groups [23]. It can be seen from figure 4c that the ZnO NPs are observed and have a spherical particle shape. The SEM image of ZnO NPs shows that the final products exhibited aggregation as a result of surface modification by the attachment of the grafted polymer.

The presence of ZnO in the textile-g-(chitosan/HEMA) can be determined by EDX analysis as supporting information, confirming the presence of ZnO in the grafted textile. Figure 5 presents the EDX curves of nano-ZnO/grafted textile. From the figure it can be clearly noticed that EDX analysis confirms the existence of Zn and O peaks of ZnO in the grafted textile.

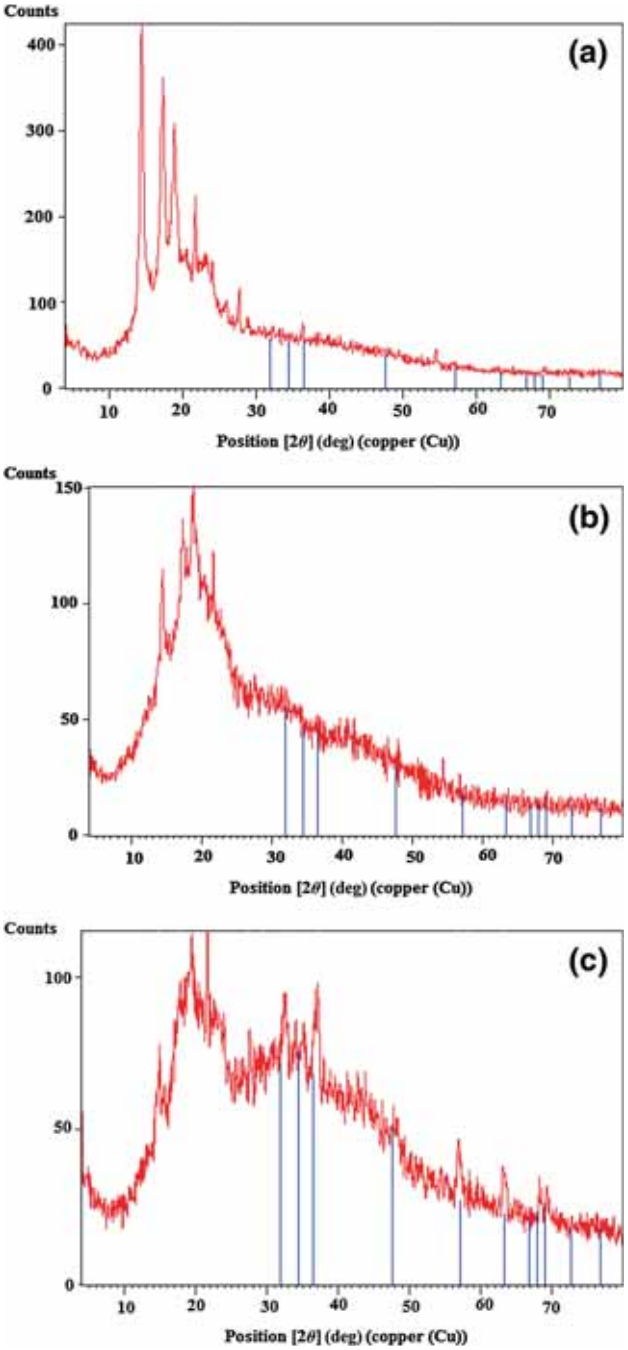

Figure 6. XRD of (**a**) plain textile, (**b**) textile-g-(chitosan/HEMA) (50:50) and (**c**) nano-ZnO/grafted textile at 20 kGy.

The XRD data of plain textile, textile-g-(chitosan/HEMA) and nano-ZnO/grafted textile are discussed to investigate some features, namely the degree of ordering and crystallite size. XRD analysis was performed also to confirm the crystal phase of ZnO NPs embedded grafted textile. Figure 6a–c shows the typical XRD pattern for the specimen. The observed peak around 2θ value of 20° corresponds to the amorphous nature of the plain textile and textile-g-(chitosan/HEMA) (figure 6a, b). It was noted that the grafting process for textile

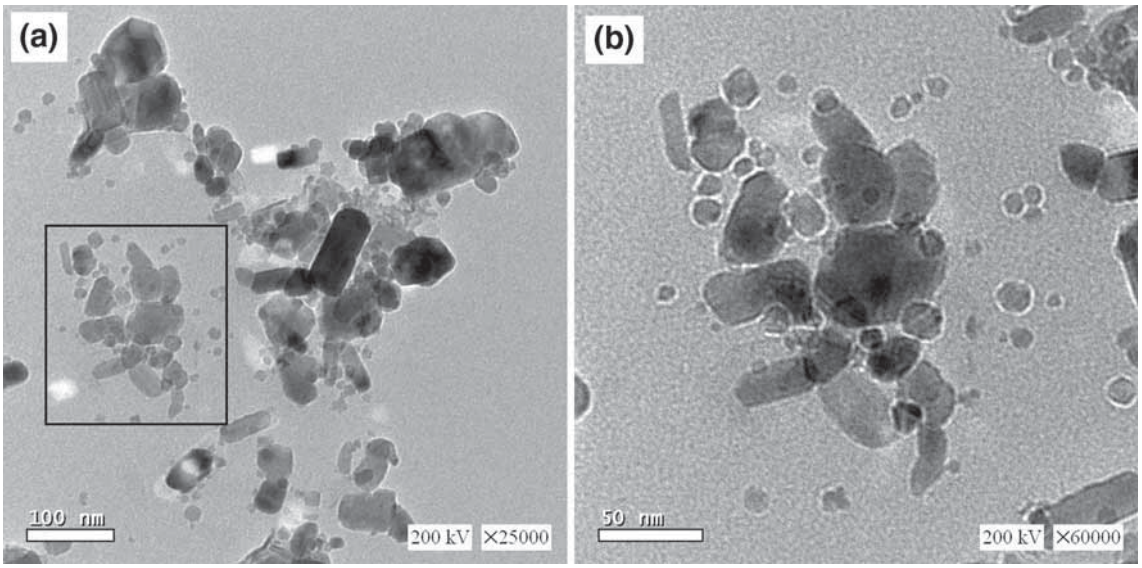

Figure 7. Typical TEM micrographs of nano-ZnO/grafted textile with different magnification power: (**a**) 25,000 and (**b**) 60,000.

Table 1. The antibacterial activity of nano-ZnO/grafted textile at different concentrations (%) against some pathogenic bacteria.

	Diameter of inhibition zone (mm)			
		Concentration of nano-ZnO/grafted textile (%)		
Tested isolates	Gentamycin	0.05	0.3	3
Staph. spp. (1)	15	9	10	15
Staph. spp. (2)	20	—	—	10
Staph. spp. (3)	22	9	9	9
Staph. spp. (4)	22	—	9	10
Staph. spp. (5)	21	9	10	13
E. coli (1)	12	9	9	10
E. coli (2)	13	—	8	8
E. coli (3)	8	—	10	12
E. spp. (4)	—	8	10	15
E. spp. (5)	—	—	9	10
K. spp. (1)	12	8	9	10
K. spp. (2)	15	—	8	10
K. spp. (3)	20	8	8	13
K. spp. (4)	—	—	10	15
K. spp. (5)	—	—	—	8
P. spp. (1)	15	—	8	12
P. spp. (2)	—	—	—	—
P. spp. (3)	17	7	9	13
Bacillus sp.	19	—	—	9

brought about a drop in the degree of ordering of the plain textile and textile-g-(chitosan/HEMA). These findings were evidenced from the observed big drop in the relative intensity of the main diffraction line and its broadening [31]. The nano-ZnO/grafted textile in figure 6c shows the peaks at 31.9, 34.6, 36.4, 47.6, 56.7, 62.9, 66.6, 68.0 and 69.2°, which can be assigned, respectively, to (100), (002), (101), (102), (110), (103), (200), (112) and (201) crystal planes of ZnO with hexagonal structure [32].

To determine the size and shape of the majority of ZnO NPs using the TEM, the particles in the grafted textile were crushed according to the procedure mentioned in the

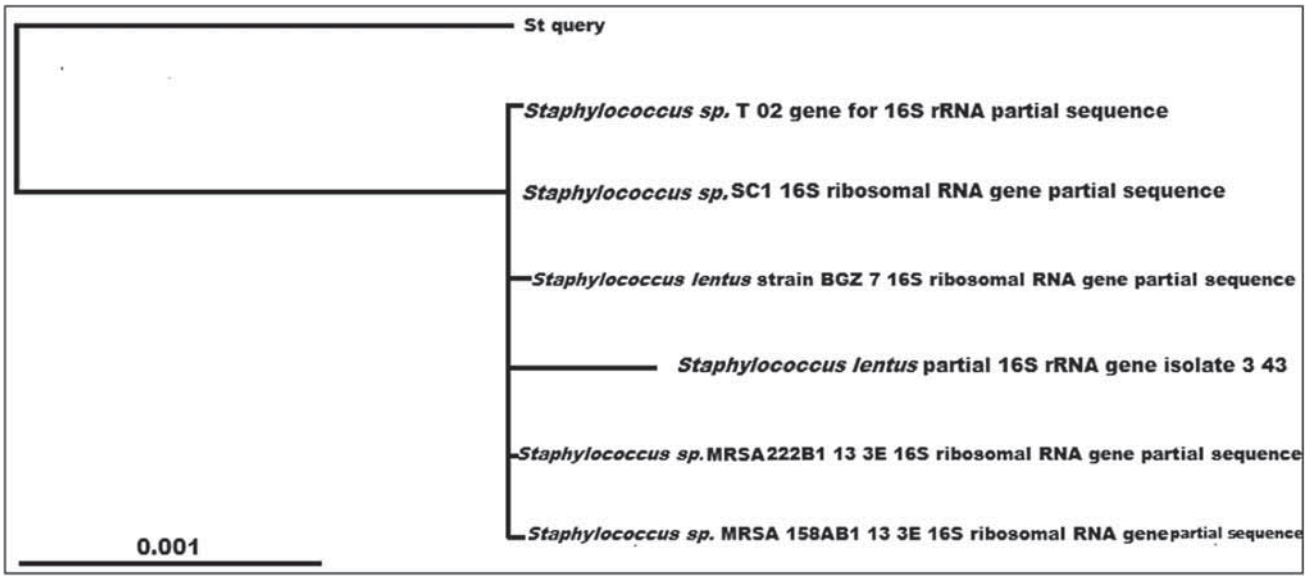

Figure 8. The phylogeny tree of *Staphylococcus* sp. PCR molecular identification.

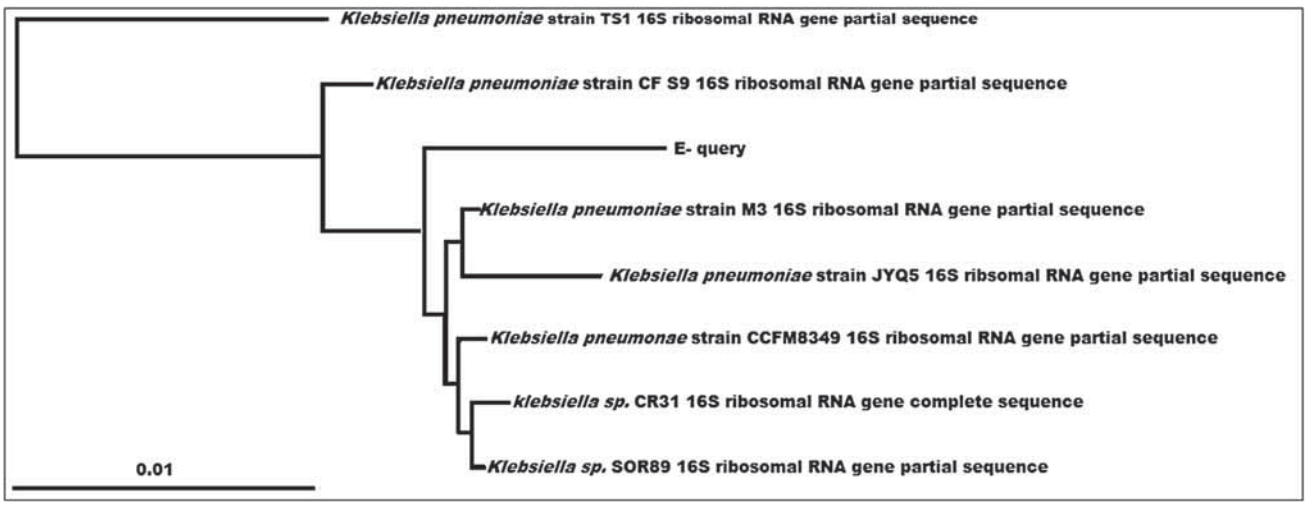

Figure 9. The phylogeny tree of *Klebsiella pneumoniae* PCR molecular identification.

experimental section and the supernatants were viewed under the TEM, which is presented in figure 7a and b. It is clear from the figure that the ZnO NPs formed in the grafted textile are partially quasispherical in shape, highly dispersed and of small nanosize. The particles mean size is found to be 10 nm in the range 6.18–17.72 nm.

3.3 *Applications*

3.3a *Assessment of the antimicrobial activity of nano-ZnO/grafted textile*: The increase of the occurrence of antibiotic resistance in the pathogenic bacteria and fungi is a matter of serious concern. The antimicrobial property of new ZnO-NPs has been found to be stable and of relatively low toxicity; hence, they are potential antimicrobial agents [7]. Consequently, one of the objectives of this study was to finish ZnO-NPs onto the textile. The antimicrobial function of nano-ZnO/grafted textile was determined qualitatively by the disk diffusion method. Gentamycin and Nystatin, as two of the most active antibacterial and antifungal agents, were used as standards. On referring to them, nano-ZnO/grafted textile showed antimicrobial action against the tested pathogens at different levels (table 1), whereas the plain textile and chitosan/HEMA-g-textile showed no antimicrobial activity (not tabulated). As mentioned in the literatures, the antibacterial properties of chitosan are due to the interaction between the positive charges of chitosan and the electronegativity charged residues of the macromolecules at the microorganism cell surface, which causes the membrane leakage [33]. This

antibacterial property has vanished due to the interaction of the positive amino groups of chitosan with negative hydroxyl groups of the HEMA during the grafting process. The tested pathogens showed an increasing inhibition zone with increasing ZnO-NP concentrations. The results also showed that, on referring to the standard antibiotics, nano-ZnO/grafted textile (3%) have a pronounced antimicrobial activity against *Staphylococcus* spp. (strain number 1) and *Klebsiella* spp. (strain number 4) with inhibition zone (15 mm) for both. Also, against *Candida* sp. the inhibition zone was 10 mm, while it was not affected by Nystatin. The antimicrobial activity of nano-ZnO/grafted textile reported against *MRSA* and *Klebsiella pneumoniae* was 18.5 and 13.5 mm diameter inhibition zone, respectively, by Singh *et al* [34]. These results and that obtained by Rajendran *et al* [35] can be correlated with our results, where a significant antibacterial activity of fabrics treated with zinc oxide against *MRSA* is demonstrated. On the other hand, regarding the antimicrobial activity of the grafted discs, our results differ from others [36]; this difference may be due to chemical modification of chitosan through the graft copolymerization.

Neighbour-joining phylogeny trees of the output result of BLAST indicated that the submitted gene corresponding to rRNA sequence is identical by 98% to *Staphylococcus* sp. MRSA222B1 13 3E 16S ribosomal RNA gene, partial sequence (figure 8) and by 97% to *K. pneumoniae* strain CF-S9 16S ribosomal RNA gene, partial sequence (figure 9) [17].

Figure 10a and b shows the antibacterial action of nano-ZnO/grafted textile quantitatively. The results indicated that, in case of plain textile the number of survivors of the applied strains increased during the 24-h contact time, while nano-ZnO/grafted textile caused decrease in the log number of survivors of *MRSA* and *K. pneumoniae* by 2 log cycles for both at the end of contact time. The antibacterial activity of ZnO NPs towards *K. pneumoniae* was studied by Brayner *et al* [37] and Sharma *et al* [38]; they observed that on contact with bacteria, the cytotoxic behaviour of ZnO NPs leads to rupture of the lipid bilayer of bacterium, resulting in leakage of cytoplasmic contents. Others suggested that this antimicrobial activity could be attributed to the generation of hydrogen

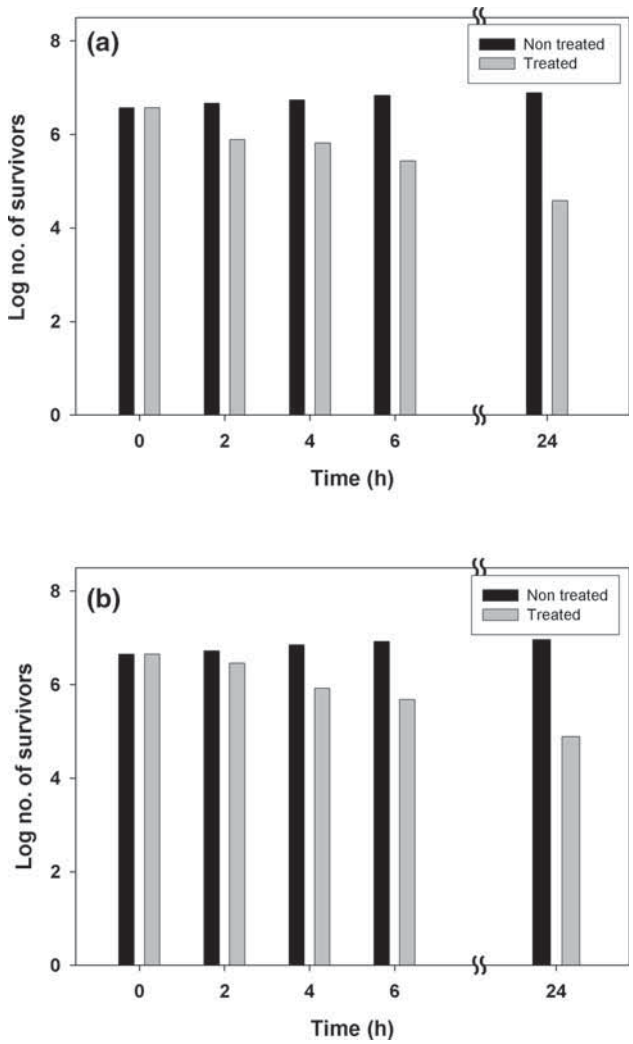

Figure 10. Effect of nano-ZnO/grafted textile (3%) at different time intervals on (**a**) *MRSA* and (**b**) *K. pneumoniae*.

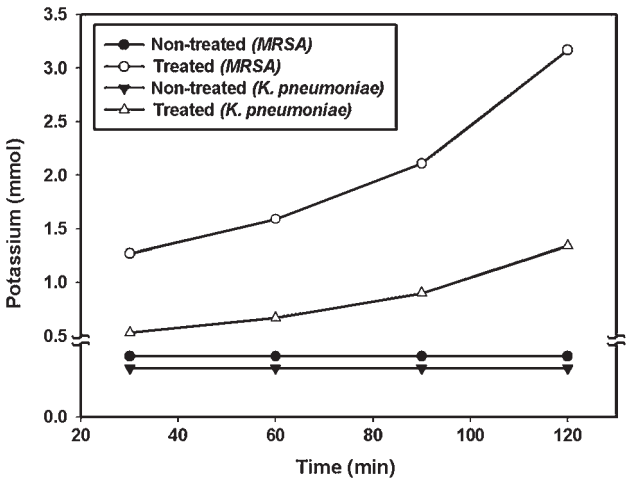

Figure 11. Effect of nano-ZnO/grafted textile on leakage of potassium ion from the tested strains for 120 min at 37°C.

Table 2. Loss of 260-nm absorbing material.

Treatment	Time (h) 2	4	6
MRSA			
Control cells	2.81	2.83	2.80
Cells treated with plain textile discs	2.80	2.81	2.81
Cells treated with nano-ZnO/grafted textile discs	3.97	4.52	4.99
K. pneumoniae			
Control cells	2.90	2.90	2.89
Cells treated with plain textile discs	2.87	2.87	2.85
Cells treated with nano-ZnO/grafted textile discs	3.60	4.08	4.72

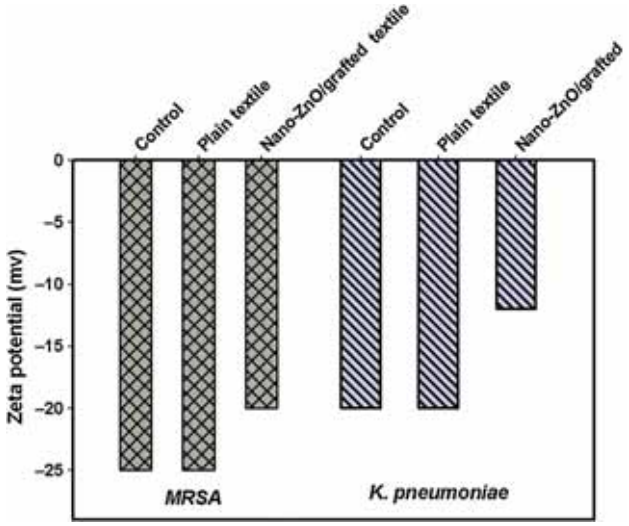

Figure 12. Bacterial surface charge-Zeta potential of tested strains treated with nano-ZnO/grafted textile.

peroxide from the surface of ZnO, which is considered as an effective means for the inhibition of bacterial growth [39]. Several studies have proposed the release of Zn^{2+} ions, which can damage the cell membrane and interact with intracellular contents [37].

To investigate the mode of action of nano-ZnO against the susceptible strains, the following tests were carried out.

3.3b *Leakage of potassium ion and 260 nm absorbing material*: The precise detection of potassium ion is crucial because it plays a leading role in membrane transport. Therefore, the effect of ZnO NPs on leakage of potassium from the selected strains is studied and shown in figure 11. The results indicated that no loss from cells treated by plain textile discs was noticed over all time intervals of the experiment, while in case of nano-ZnO/grafted textile discs, the loss of potassium ion increased with the evaluated intervals. Another strategy for determining the mode of action was based on the release of cell constituents determined by the measurements of absorbance at 260 nm. The increase of ODs reading of the cells treated with ZnO-NP discs, compared with that in case of plain discs (table 2), shows its ability to damage the cytoplasmic membrane, and ZnO NPs rupture the lipid bilayer of bacterium, resulting in leakage of cytoplasmic contents [38].

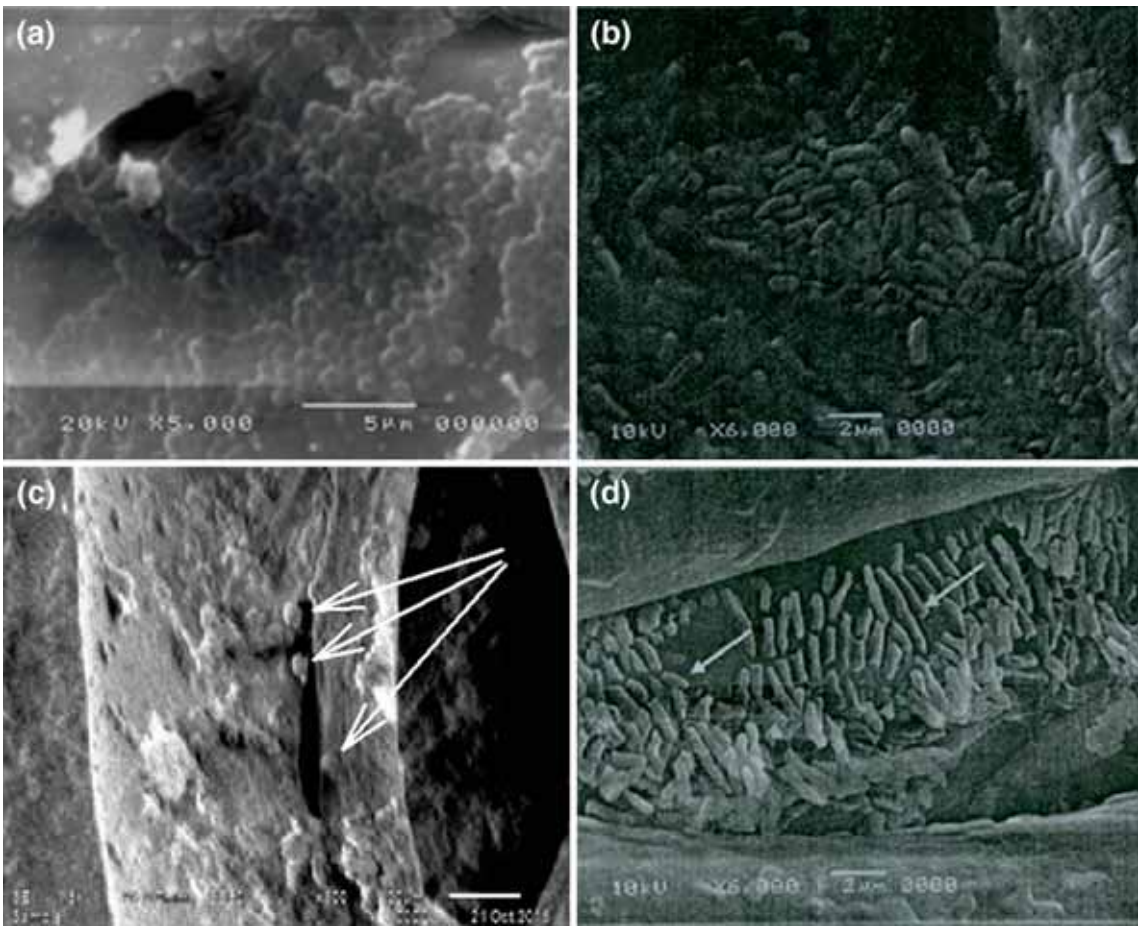

Figure 13. SEM images of *MRSA* and *K. pneumonia* grown on (**a** and **b**) plain textile and (**c** and **d**) nano-ZnO/grafted textile.

Zeta potential measurements are carried out to examine the effect of ZnO NPs on the membrane surface potential. As shown in figure 12, the bacterial cells with plain textile discs display zeta potential of −25 and −20 mV for *MRSA* and *K. pneumoniae*, respectively. However the zeta potential decreased after contact with nano-ZnO/grafted textile discs. Our results are in agreement with another study performed by Arakha *et al* [40]. This emphasizes the capability of NPs to destabilize the bacterial membrane as a result of electrostatic interaction between nano-ZnO/grafted textile, which contain +ve charge in water suspension, and bacterial cell surface (negatively charged). Such reverse charges enhance the total effect by creating electrostatic forces, which serve as a powerful bond between ZnO NPs and bacterial surface, causing cell membrane damage [7,41].

3.3c *SEM study*: Figure 13 (plates a and b) presents the morphology, respectively, of *MRSA* and *K. pneumoniae* grown on plain discs, with a huge number of cells observed by SEM. On the other hand, plates c and d show smaller number of deformed cells grown on nano-ZnO/grafted textile discs.

4. Conclusion

In this study, ZnO NPs were successfully stabilized in textile-g-(chitosan/HEMA) by gamma radiation. The grafting and swelling percent are significantly influenced by the copolymer composition and irradiation dose. The EDX analysis confirms the existence of Zn and O peaks of ZnO in the grafted textile. The X-ray data confirm the crystal phase of ZnO NPs embedded in the grafted textile as a hexagonal structure. The TEM analysis proved that the ZnO NPs were well dispersed in the grafted textile with mean size of 10 nm in the range 6.18–17.72 nm. The nano-ZnO/grafted textile with different ZnO concentrations was tested for its antimicrobial activity against 20 clinical isolates. The results revealed that nano-ZnO/grafted textile (3%) showed a pronounced antimicrobial action at different levels. The most susceptible isolates were identified genetically as 16S rRNA of *MRSA* and *K. pneumoniae*. The number of survivors of the two strains decreased by two log cycles during 24 h contact time. Loss of potassium ion and release of cell constituents at 260 nm, observed in case of nano-ZnO/grafted textile, and decrease of membrane surface potential, determined by measurements of zeta potential, demonstrate its ability to damage the cytoplasmic membrane. The SEM examination of cells grown on nano-ZnO/textile showed a decrease in the number of cells with deformation in the cells. These results are promising in the antimicrobial field.

References

[1] Tinker K 2010 Moment of truth: proper air flow critical to healthcare laundries *A white paper from the Healthcare Laundry Accreditation Council*

[2] Rattanawaleedirojin P, Saengiettiyut K and Sangsuk S 2008 *J. Nat. Sci.* **7** 75

[3] Gupta P, Bajpai M and Bajpai S K 2008 *J. Cotton Sci.* **12** 280

[4] Vinosova J and Vavrikova E 2008 *Curr. Pharm. Des.* **14** 1311

[5] Fu L, Liu Z, Liu Y, Hu P, Cao L and Zhu D 2005 *Adv. Mater.* **17** 217

[6] Makhluf S, Dror R, Nitzan Y, Abramovich Y, Jelnek R and Gedanken A 2005 *Adv. Funct. Mater.* **15** 1708

[7] Stoimenov P K, Klinger R L, Marchin G L and Klabunde K J 2002 *Langmuir* **18** 6679

[8] Holister P, Weener J W, Vas C R and Harper T 2003 *Nanoparticles: technology white papers 3* (London: Cientific Ltd.)

[9] Martinez-Gutierrez F, Olive P L, Banuelos A, Orrantia E, Nino N, Sanchez E M *et al* 2010 *Nanomedicine* **6** 681

[10] Gao Y and Cranston R 2008 *Text. Res. J.* **78** 60

[11] Chen C Y and Chiang C L 2008 *Mater. Lett.* **62** 3607

[12] Duran N, Marcarto P D, De Souza G I H, Alves O L and Esposito E 2007 *J. Biomed. Nanotechnol.* **3** 203

[13] Sawai J, Kawada E, Kanou F, Igarashi H, Hashimoto A, Kokugan T *et al* 1996 *J. Chem. Eng. Jpn.* **29** 627

[14] Huang Z, Zheng X, Yan D, Yin G, Liao X, Kang Y *et al* 2008 *Langmuir* **24** 4140

[15] Zhang L, Jiang Y, Ding Y *et al* 2007 *J. Nanopart. Res.* **9** 479

[16] Ophori E A and Wemabu E C 2010 *Nigeria. Afr. J. Microbiol. Res.* **4** 1719

[17] James G 2010 In: M Schuller, T P Sloots, G S James, C L Halliday and I W J Carter (eds) *PCR for clinical microbiology* ISBN: 978-90-481-9038-6 (Netherlands: Springer) p 209

[18] AATCC Committee RA31 1961 *Antibacterial finishes on textile materials: assessment of AATCC Test Method 100-2004 developed in 1961*

[19] Eid M and Araby E 2013 *Appl. Biochem. Biotechnol.* **171** 469

[20] Halder S, Yadava K K, Sarkar R, Mukherjee S, Saha P, Halder S *et al* 2015 *Springerplus* **4** 672

[21] Ali A E H, Shawky H A, El Rehim H A A and Hegazy E A 2003 *Eur. Polym. J.* **39** 2337

[22] Taher N H, Dessouki A M and El-Arnaouty M B 1998 *Radiat. Phys. Chem.* **53** 437

[23] El-Arnaouty M B, El-Kelesh N A and Abdel-Aal S E 2004 *Arab. J. Nucl. Sci. Appl.* **37** 17

[24] El-Arnaouty M B, Abedel Ghaffar A M and El-Shafey H M 2008 *J. Appl. Polym. Sci.* **107** 744

[25] Taher N H, El-Sayed A H, Dessouki A M and El-Arnaouty M B 1989 *Int. J. Radiat. Appl. Instrum. C Radiat. Phys. Chem.* **33** 129

[26] El-Hag A A and Al-Arifi A 2009 *Carbohydr. Polym.* **78** 725

[27] Lanthong P, Nuish R and Kiatkamjornwong S 2006 *Carbohydr. Polym.* **66** 229

[28] Fang J M, Fowler P A, Sayers C and Williams P A 2004 *Carbohydr. Polym.* **55** 283

[29] Wang P, Wu X, Xue D, Xu K, Tan Y, Du X and Li W 2009 *Carbohydr. Res.* **344** 851

[30] Fan L, Luo C, Zhen L, Fuguang L and Qiu H 2011 *Colloids Surf. B Biointerfaces* **88** 574

[31] Atia K S, Al-Arnaouty M B, Ismail S A and Dessouki A M 2003 *J. Appl. Polym. Sci.* **90** 155

[32] Salehi R, Arami M, Mahmodi N M, Bahrami H and Kharramfor S 2010 *Colloid Surf. B* **80** 86

[33] Begin A and Van Calsteren M R 1999 *Int. J. Biol. Macromol.* **26** 63
[34] Singh G, Joyce M E, Beddow J and Mason J T 2012 *J. Microbiol. Biotechnol. Food Sci.* **2** 106
[35] Rajendram R, Balakumar C, Ahammed M A H, Jaya Kumar S, Vaideki K and Rajesh E M 2010 *Int. J. Eng. Sci. Technol.* **2** 202
[36] Ignatova M, Manolova N and Rashkov I 2007 *Eur. Polym. J.* **43** 1112
[37] Brayner R, Ferrari-Iliou R, Brivois N, Djediat S, Benedetti M F and Fievet F 2006 *Nano Lett.* **6** 866
[38] Sharma D, Rajput J, Kaith B S, Kaur M and Sharma S 2010 *Thin Solid Films* **519** 1224
[39] Yamamoto O 2001 *Int. J. Inorg. Mater.* **3** 643
[40] Arakha M, Saleem M, Mallick C B and Jha S 2015 *Scientific Rep.* **5** 9578
[41] Zhang L, Ding Y, Povey M and York D 2008 *Prog. Nat. Sci.* **18** 939